1 Final Technical Report: Vibrational Spectroscopy of Transient Combustion Intermediates Trapped in Helium Nanodroplets

1.1 DE-SC0008086

11/16/2017 Gary E. Douberly

1.1.1 Spectroscopy of Combustion Intermediates in Superfluid Helium Droplets

The objective of our experimental research program is to isolate and stabilize transient intermediates and products of prototype combustion reactions. This will be accomplished by Helium Nanodroplet Isolation (HENDI),[1–6] a novel technique where liquid helium droplets freeze out high energy metastable configurations of a reacting system, permitting infrared (IR) spectroscopic characterizations of products and intermediates that result from hydrocarbon radical reactions with molecular oxygen and other small molecules relevant to combustion environments (see Refs. 7–39 for our recent contributions applying this method). The low temperature (0.4 K) and rapid cooling associated with He droplets provides a perfectly suited medium to isolate and probe a broad range of molecular radical and carbene systems important to combustion chemistry. The sequential addition of molecular species to He droplets often leads to the stabilization of high-energy, metastable cluster configurations that represent regions of the potential energy surface far from the global minimum. Single and double resonance IR laser spectroscopy techniques, along with Stark and Zeeman capabilities, are being used to probe the structural and dynamical properties of these systems.

A diagram of the HENDI apparatus is shown in Fig. 1. Helium droplets are formed (10^{12} droplets per second) by the continuous expansion of He gas through a 5 micron diameter pinhole nozzle (Fig. 1A). The average droplet size is controlled by changing the nozzle temperature, providing a dynamic range from $\sim 10^3$ atoms at 24 K to $\sim 10^6$ atoms at 8 K.[40–43] Upon leaving the high pressure region of the expansion, the droplets cool by evaporation to 0.4 K.[44] The droplet expansion is skimmed into a beam, which passes into the differentially pumped pick-up chamber (Fig. 1B). Here the droplets are doped by passing them through the vapor of the molecular species of interest (approximately 10^{10} molecules/cm^3 over a 1 cm path length). The internal energy of the captured molecule is rapidly removed by He evaporation, which returns the system to 0.4 K.[45] Each evaporating He atom reduces the internal energy of the system by 5 cm^{-1} (0.014 kcal mol^{-1}).[45] The density of molecules in the "pick-up" region can be varied such that each droplet captures one (or more) molecules on average. Molecular species of differing composition can be added to the

same droplet by implementing multiple "pick-up" zones. An effusive pyrolysis source (Fig. 2) has been successfully used by us to fragment precursor molecules and dope He droplets with halogen atoms and molecular radicals or carbenes.[11,12,14–17,19,21,23,24,28,29,31–36]

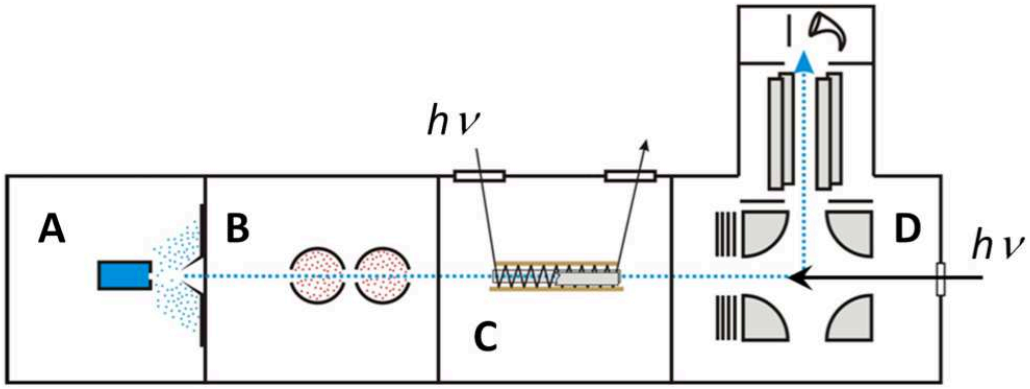

Figure 1: Schematic of the UGA HENDI spectrometer. The pyrolysis source for generating halogen atoms and molecular radicals or carbenes is load-locked into the vacuum chamber (section B). The laser excitation can be switched between a counter-propagating configuration to the laser-multipass/Stark cell configuration (section C). Detection of the droplet beam is achieved with a crossed-beam ionizer quadrupole mass spectrometer (section D).

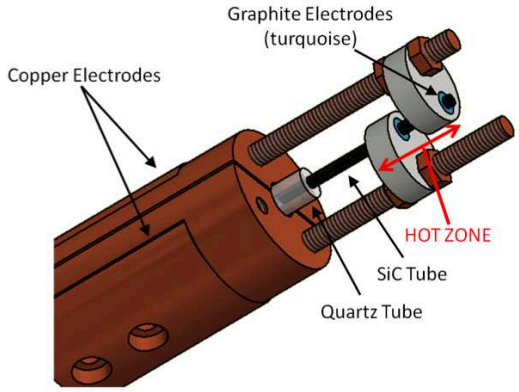

Figure 2: A schematic drawing of our SiC high temperature pyrolysis source. The copper electrodes are water-cooled and the length of the hot zone can be adjusted.

The droplet beam is detected with a quadrupole mass spectrometer (MS) (Fig. 1D). Electron impact ionization leads to the production of a He^+ cation within the droplet. The outcome of this ionization process is now well known to produce either a He_n^+ distribution or ions associated with the charge-transfer ionization and fragmentation of the molecular dopant.[1,2] The MS in Fig. 3A shows the He_n^+ ions associated with the electron impact ionization of a neat (dopant free) droplet beam. Figure 3B shows the MS of a droplet beam doped with *n*-butyl nitrite (one molecule is captured per droplet, on average; the energized molecular ion fragments predominately to $C_3H_3^+$). Thermal dissociation of *n*-butyl nitrite in a pyrolysis source leads to the production of the propargyl

radical, NO, and formaldehyde. Figure 3C shows the MS of the droplet beam after having captured the molecular fragments associated with this *n*-butyl nitrite pyrolysis. The peak at m/z=38 is a signature of the ionization and fragmentation of the He-solvated C_3H_3 radical.

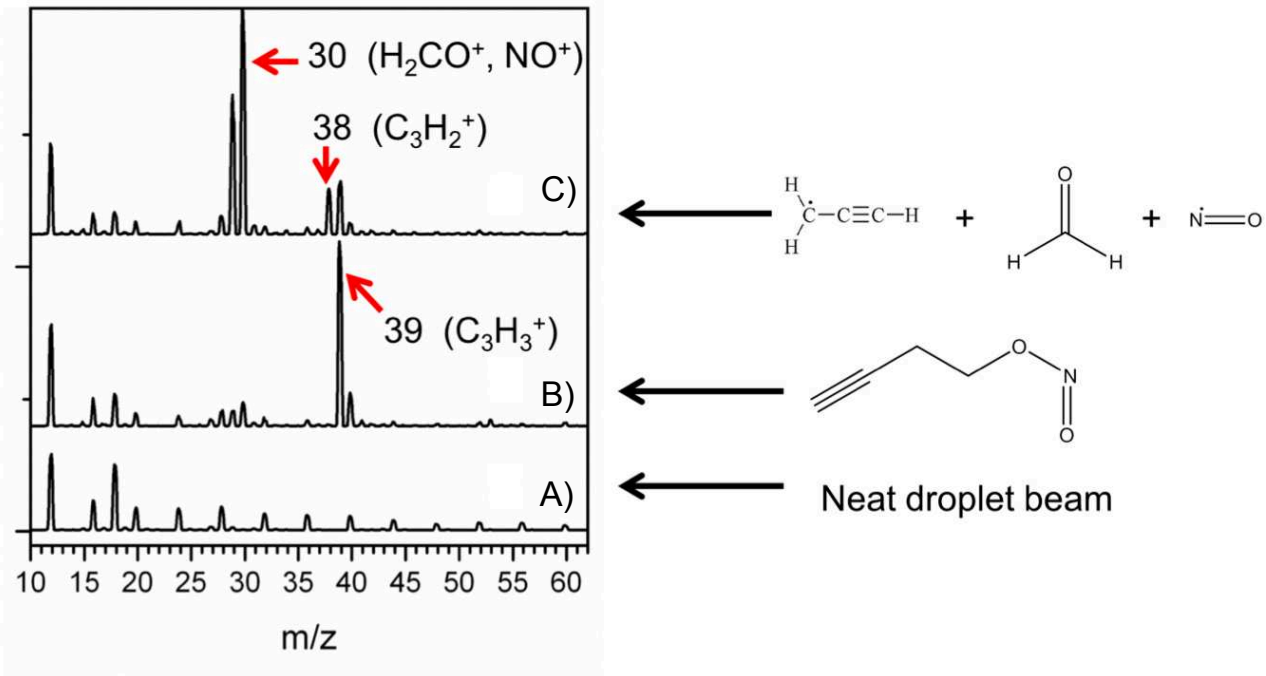

Figure 3: A) MS of the neat droplet beam. B) MS of droplets doped with single *n*-butyl nitrite molecules. C) MS of droplets doped with single molecules, NO, formaldehyde, or the propargyl radical, C_3H_3.

After traversing the pick-up zones and prior to entering the mass spectrometer, the beam of droplets is irradiated with the idler output from a continuous-wave optical parametric oscillator (OPO). Survey spectra are recorded with the laser beam aligned counter-propagating to the droplet beam, whereas the laser is aligned into a two-mirror multipass cell for Zeeman, Stark and Polarization spectroscopy measurements. Vibrational excitation of He-solvated dopants leads to the evaporation of several hundred He atoms, which reduces both the geometric and ionization cross sections of the irradiated droplets. This photo-induced cross section reduction for electron impact ionization is measured as ion signal depletion in selected mass channels. For example, the IR spectrum of *n*-butyl nitrite is measured as a depletion signal in mass channel m/z=39 (Fig. 4A; experimental conditions same as those in Fig. 3B), whereas the spectrum of the propargyl radical is measured in mass channel m/z=38 (Fig. 4B; experimental conditions same as those in Fig. 3C). As demonstrated in Fig. 4B, mass channels can be judiciously selected so as to discriminate against spectral features associated with droplets containing unpyrolyzed precursor molecules

or other fragments of pyrolysis. The weakly perturbing, superfluid He solvent allows for highly resolved vibrational spectroscopy studies of these species that can be compared directly to the predictions of quantum chemistry.[1,2] Indeed, in the case of vibrational frequencies, when comparisons are available, the band origins of He-solvated molecules and molecular complexes differ little from those measured in the gas phase ($\sim$1 cm^{-1} or less).[1] All of these aspects of HENDI are perfectly suited for the pick-up and spectroscopic interrogation of the molecular systems discussed in this proposal.

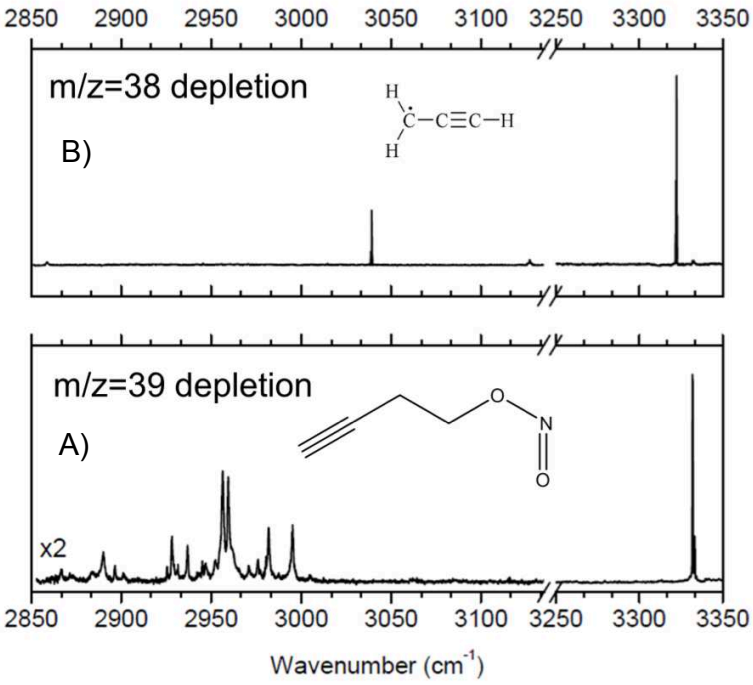

Figure 4: Infrared spectra of (A) *n*-butyl nitrite and (B) the propargyl radical measured as ion signal depletion in mass channels 39 and 38 u, respectively.

For small molecules and molecular complexes assembled in He droplets, it is often the case that vibrational bands exhibit rotational fine structure. The rotationally resolved spectra can be analyzed with an effective Hamiltonian approach, in which the gas-phase Hamiltonian is used with renormalized rotational constants. Stark spectroscopy can therefore be used in the traditional sense, in which an external electric field perturbs the free-rotor behavior of the molecule or complex. Our instrument is equipped with a laser multipass cell (Fig. 1C) that allows us to perform Stark spectroscopy measurements by applying a static electric field (0 to 80 kV/cm) to electrodes that surround the droplet beam/laser interaction region. The use of various Stark field strengths and laser polarization orientations (leading to different selection rules), allows us to accurately determine

dipole moments of He-solvated species.[15,35,46,47] For example, the experimental and simulated Stark spectra of the OH–C_2H_2 complex are shown in Fig. 7 in Section 1.1.5.[35]

Often, the natural line width due to vibrational relaxation is broader than the rotational contour at 0.4 K ($\sim$1 cm^{-1}), precluding the determination of dipole moments *via* the aforementioned Stark measurements. This is a common feature for larger He-solvated systems that have a relatively high density of vibrational states, leading to more efficient coupling to the solvent and more rapid vibrational relaxation.[1,7,8,48,49] Nevertheless, by measuring the electric field dependence of the band intensity, it is possible to simultaneously obtain both the permanent electric dipole moment (μ_p) and the vibrational transition moment angle (VTMA)[8,48,50] associated with each vibrational band.[50,51] For any one normal mode vibration, the VTMA is defined as the angle μ_p makes with the transition dipole moment vector (μ_t). Given a particular combination of VTMA and μ_p (obtained from *ab initio* calculations), this field dependence can be simulated and compared to the experiment.[52–54] Moreover, to make this comparison, the theoretical results do not require the scaling that often plagues the comparisons of experimental vibrational band origins to those obtained from *ab initio* harmonic frequency calculations.[50] Because dipole moments and VTMAs are accurately determined even at modest levels of *ab initio* theory, these *Polarization Spectroscopy* measurements provide key structural information that can be employed to assign vibrational spectra that contain contributions from multiple species or structural isomers.[50]

Research Highlights

1.1.2 Infrared Spectroscopy of Hydrocarbon Radicals

Thermal decomposition of organic precursors in a continuous, effusive pyrolysis source allows for the helium nanodroplet isolation (HENDI) and spectroscopic interrogation of a variety of hydrocarbon radicals (see Section 1.1.1 for a detailed description of the HENDI methodology). Many of these initial studies involved small radicals that had been spectroscopically probed in the gas phase. Nevertheless, as summarized here, the low temperature afforded by He droplets allows for a characterization of these systems beyond what has so far been achieved in the gas phase. More recent studies of larger radical systems that have yet to be spectroscopically probed in the gas phase are encouraging (*e.g.* propyl radicals),[39] as it seems the only limitation to the HENDI method is the availability of suitable pyrolysis precursors.

Helium-Mediated Tunneling Dynamics of the Vinyl Radical

The vinyl radical (H_2C_β =C_αH) was produced *via* the pyrolysis of di-vinyl sulfone and trapped in liquid He droplets.[24] At 0.4 K, the entire population of nuclear spin isomers is cooled to either the 0_{00}^+ (ortho) or 0_{00}^- (para) rotovibrational level. IR spectra in the fundamental CH stretch region revealed three bands that we assigned to the symmetric CH_2 (ν_3), antisymmetric CH_2 (ν_2) and lone α–CH (ν_1) stretch bands. The vinyl radical CH stretch band origins in He droplets differ from vibrational configuration interaction calculations[55] of J. Bowman and co-workers by ∼1, 2 and 10 cm^1 for the ν_3, ν_2 and ν_1 modes, respectively. Each band consists of *a*-type and *b*-type transitions from the 0_{00} level, and each of these is split by either the *difference in* or *sum of* the $v = 0$ and $v = 1$ tunneling splittings. Comparing the He droplet spectra to previous high-resolution spectroscopy of the ν_3 band (D.J. Nesbitt and co-workers),[56,57] we found that the $A' - B'$ rotational constant for this mode is reduced to 89% of its gas-phase value, and the tunneling splittings (ground and ν_3 excited states) are both reduced by ∼20%. In addition, the relative intensities of the ν_3 transitions indicate 4:4 spin statistics for ortho and para nuclear spin isomers, suggesting a facile interchange mechanism[58] for all three H atoms within the ∼1200 K pyrolysis source, prior to the pick-up and cooling of the hot vinyl radical by the He droplet. The ∼20% reduction in the ground and ν_3 excited state tunneling splittings is due to two contributing effects from the He solvent. The He droplet can modify both the tunneling barrier and the effective reduced mass for motion along this coordinate. We have estimated that either an ∼40 cm^{-1} increase in the effective barrier height or an ∼5% increase in the effective mass of the tunneling particles (both as upper limits) is sufficient to account for the observed ∼20% tunneling splitting reduction. Future theoretical work will be required to assess the extent to which each of these effects contribute to the overall modification of the vinyl radical tunneling dynamics upon solvation in liquid He.

Methyl, Ethyl, Propargyl, Allyl, and Propyl Radicals

The methyl (CH_3) and ethyl (C_2H_5) radicals were produced *via* the pyrolysis of peroxide precursors and isolated and spectroscopically characterized in He droplets.[19,21] The five fundamental CH stretch bands of C_2H_5 near 3 μm were each observed within 1 cm^{-1} of the band origins reported for the gas phase species (D.J. Nesbitt and co-workers).[59,60] The symmetric CH_2 stretching band (ν_1) is rotationally resolved, revealing nuclear spin statistical weights predicted by G_{12} permutation-inversion group theory. The ethyl radical's permanent electric dipole moment (0.28(2) D) was

obtained *via* the Stark spectrum of the ν_1 band. Three a_1' overtone/combination bands were also observed, each having resolved rotational substructure. These were assigned to $2\nu_{12}$, $\nu_4+\nu_6$, and $2\nu_6$ through comparisons to anharmonic frequency computations at the CCSD(T)/cc-pVTZ level of theory and *via* an analysis of the rotational substructure observed for each band.

Rotationally resolved IR spectra were obtained for the propargyl (C_3H_3) and allyl radicals (C_3H_5).[14,17] In the IR spectrum of He-solvated allyl, we observed rovibrational bands near the band origins previously reported in high resolution gas-phase studies carried out by D.J. Nesbitt and co-workers[61] and R. Curl and co-workers.[62–64] In addition to the fundamental CH stretching modes, four other bands were assigned to the allyl radical using a consistent set of rotational constants. Indeed, in the gas-phase studies, it was noted that the CH stretch bands are heavily perturbed, but no explanation was given as to the nature of the perturbations. Isolating the radical in He droplets greatly decreases the number of populated rovibrational levels, and aided by anharmonic frequency computations and the resolved rotational substructure, we assigned the ν_1 (a_1), ν_3 (a_1), ν_{13} (b_2) fundamentals and the $\nu_{14}/(\nu_{15}+2\nu_{11})$ (b_2) and $\nu_2/(\nu_4+2\nu_{11})$ (a_1) Fermi dyads, in addition to an unassigned resonant polyad near the ν_1 mode.

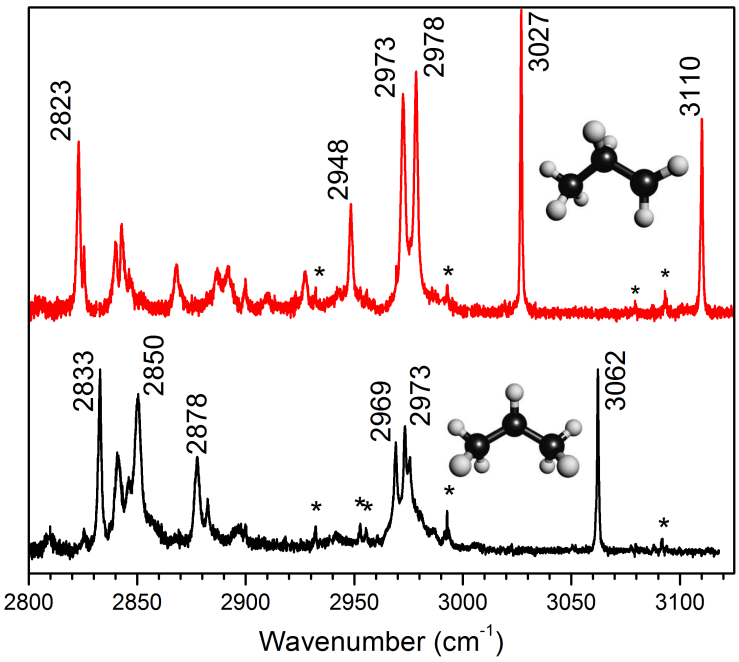

Figure 5: Comparison of the IR spectra of *n*-propyl (top, red) and *i*-propyl radicals (bottom, black). All vibrational bands are broadened beyond the rotational contour expected at 0.4 K. Residual propene absorptions are marked by *.

In our most recent work,[39] gas-phase *n*-propyl and *i*-propyl radicals (C_3H_7) were generated *via* pyrolysis of *n*-butyl nitrite and *i*-butyl nitrite, respectively. An Ar-matrix isolation study from

the late 1970s represents the only previous molecular spectroscopy of these radicals.[65,66] Several previously unreported bands were observed in the IR spectrum between 2800 and 3150 cm^{-1} (Fig. 5). The CH stretching modes observed above 2960 cm^{-1} are in excellent agreement with anharmonic frequencies computed using second-order vibrational perturbation theory. However, between 2800 and 2960 cm^{-1}, the spectra of *n*- and *i*-propyl radicals become congested and difficult to assign due to the presence of multiple anharmonic resonances. Computations employing a local mode Hamiltonian reveal the origin of the spectral congestion to be strong coupling between the high frequency CH stretching modes and the lower frequency bending/scissoring motions. The most significant coupling is between stretches and bends localized on the same CH_2/CH_3 group. This work was carried out as a collaboration between the experiment/theory groups at the University of Georgia and Edwin L. Sibert at the University of Wisconsin-Madison.

Infrared Spectroscopy of Cyclobutyl, Methylallyl, and Allylcarbinyl Radicals

Gas phase cyclobutyl radical ($^{\bullet}C_4H_7$) were produced *via* pyrolysis of cyclobutylmethyl nitrite ($C_4H_7(CH_2)ONO$). Other $^{\bullet}C_4H_7$ radicals, such as 1-methylallyl and allylcarbinyl, are similarly produced from nitrite precursors. Nascent radicals are promptly solvated in liquid He droplets, allowing for the acquisition of infrared spectra in the CH stretching region. For the cyclobutyl and 1-methylallyl radicals, anharmonic frequencies are predicted by VPT2+K simulations based upon a hybrid CCSD(T) force field with quadratic (cubic and quartic) force constants computed using the ANO1 (ANO0) basis set. A density functional theoretical method is used to compute the force field for the allylcarbinyl radical. For all $^{\bullet}C_4H_7$ radicals, resonance polyads in the 2800-3000 cm^{-1} region appear as a result of anharmonic coupling between the CH stretching fundamentals and CH_2 bend overtones and combinations. Upon pyrolysis of the cyclobutylmethyl nitrite precursor to produce the cyclobutyl radical, an approximately two-fold increase in the source temperature leads to the appearance of spectral signatures that can be assigned to 1-methylallyl and 1,3-butadiene. On the basis of a previously reported $^{\bullet}C_4H_7$ potential energy surface, this result is interpreted as evidence for the unimolecular decomposition of the cyclobutyl radical *via* ring opening, prior to it being captured by helium droplets. On the $^{\bullet}C_4H_7$ potential surface, 1,3-butadiene is formed from cyclobutyl ring opening and H atom loss, and the 1-methylallyl radical is the most energetically stable intermediate along the decomposition pathway. The allylcarbinyl radical is a higher energy $^{\bullet}C_4H_7$ intermediate along the ring opening path, and the spectral signatures of this radical are

not observed under the same conditions that produce 1-methylallyl and 1,3-butadiene from the unimolecular decomposition of cyclobutyl.

1.1.3 R· + $(^3\Sigma_g^-)O_2$ Chemistry in Helium Droplets

Methyl Peroxy Radical

We have demonstrated that R· + $(^3\Sigma_g^-)O_2$ reactions can be carried out within the low temperature, He droplet environment. For example, the sequential addition of a methyl radical and molecular oxygen to He droplets leads to the barrierless reaction, $CH_3 + O_2 \rightarrow CH_3OO$.[11] The reaction enthalpy is exothermic by ∼30 kcal mol^{-1} and therefore requires the dissipation of ∼2000 He atoms to cool CH_3OO to 0.4 K. The CH_3OO radical remains in the droplet and is observed downstream with IR laser beam depletion spectroscopy. All three CH stretch bands are observed, and rotational fine structure is partially resolved for the ν_2 totally symmetric CH stretch band, indicating complete internal cooling of the reaction product to the droplet temperature. Electron impact ionization of the droplets containing CH_3OO results in the charge transfer reaction $He^+ + CH_3OO \rightarrow CH_3O_2^+ + He$, which is followed by the fragmentation of the $CH_3O_2^+$ ion. The major fragmentation channel is the production of HCO^+ and H_2O. The outcome of this work demonstrates that IR laser spectroscopy can be employed as a probe of the outcome of organic radical-radical reactions carried out in the dissipative environment of a He nanodroplet.

Propargyl and Allyl Peroxy Radicals

IR spectroscopy was used to probe the outcome of the reaction between the propargyl radical (C_3H_3) and $(^3\Sigma_g^-)O_2$ within He droplets.[17] Helium droplets doped with a propargyl radical (generated *via* pyrolysis of 1-butyn-4-nitrite) were subsequently doped with an O_2 molecule. The reaction carried out at 0.4 K resulted in the exclusive formation of the acetylenic-*trans*-propargyl peroxy radical ($HC{\equiv}C–CH_2–OO^{\bullet}$). This work helped to elucidate the shape of the entrance channel on the ground-state potential energy surface, as it was unclear whether or not there exists a small barrier to formation of the peroxy species. The rapid cooling afforded by the He droplets motivates the conclusion that if a barrier does indeed exist, it is too small to kinetically stabilize a van der Waals complex between C_3H_3 and O_2. MRCI computations carried out in collaboration with Stephen Klippenstein and co-workers indicate that the reaction is barrierless for O_2 addition to the

–CH_2 "tail" group, similar to alkyl + O_2 reactions. Apparently, O_2 addition to the HC≡C– "head" group proceeds *via* a positive entrance channel barrier, consistent with the absence of *allenic* peroxy radicals in the He droplet IR spectra.

Five stable conformers were predicted for the allyl peroxy radical (H_2C=$CHCH_2$–$OO^\bullet$).[67] A two-dimensional potential surface was computed for rotation about the CC–OO and CC–CO bonds,[14] revealing multiple isomerization barriers greater than ∼300 cm^{-1}. Nevertheless, the CH stretch IR spectrum can be assigned assuming the presence of a *single* conformer following the allyl + O_2 reaction within He droplets.[14] This is similar to the observation for the propargyl peroxy system, and from this we can infer a cooling mechanism for the vibrationally hot reaction products (R–$OO^\bullet$) that is consistent with both sets of data. The mechanism assumes that the more closely spaced torsional levels (<100 cm^1) are relaxed more efficiently by the He solvent in comparison to the higher frequency vibrations, allowing the system to funnel into the lowest energy conformational minimum as it cascades down the ladder of excited stretching/bending levels.

1.1.4 Infrared Spectroscopy of Hydroxycarbenes

Hydroxymethlyene, Dihydroxycarbene, Hydroxymethoxycarbene

Hydroxymethylene (HC̈OH) and its d_1-isotopologue (HC̈OD) were isolated in He droplets following the pyrolysis of glyoxylic acid.[26] Transitions identified in the IR spectrum were assigned exclusively to the *trans*-conformation based on previously reported anharmonic frequency computations.[68,69] For the OH(D) and CH stretches, *a*- and *b*-type transitions were observed, and when taken in conjunction with CCSD(T)/cc-pVTZ computations, lower limits to the vibrational band origins were determined. The relative intensities of the *a*- and *b*-type transitions provide the orientation of the transition dipole moment in the inertial frame. The He droplet data are in excellent agreement with anharmonic frequency computations carried out in collaboration with John F. Stanton, confirming strong anharmonic resonance interactions in the high-frequency stretch regions of the mid-IR. Moreover, the He droplet spectra confirm appreciable Ar-matrix shifts of the OH and OD stretches, which were previously postulated by Schreiner and co-workers.[68]

Dihydroxycarbene (HOC̈OH) was produced *via* pyrolytic decomposition of oxalic acid, captured by He droplets, and probed with IR laser Stark spectroscopy.[29] Rovibrational bands in the OH stretch region were assigned to either *trans*,*trans*- or *trans*,*cis*- rotamers on the basis of symmetry type, nuclear spin statistical weights, and comparisons to electronic structure theory calculations

(Fig. 6). The inertial components of the permanent electric dipole moments for these rotamers were determined with Stark spectroscopy. The dipole components for *trans,trans-* and *trans,cis-* rotamers are (μ_a, μ_b) = (0.00, 0.68(6)) and (1.63(3), 1.50(5)), respectively. The IR spectra lack evidence for the higher energy *cis,cis-* rotamer, which is consistent with a previously proposed pyrolytic decomposition mechanism of oxalic acid[70–73] and computations of HOC̈OH torsional interconversion and tautomerization barriers.[74]

Hydroxymethoxycarbene ($CH_3O\ddot{C}OH$) was similarly produced *via* monomethyl oxalate pyrolysis.[30] Two rotationally resolved *a,b-* hybrid bands in the OH-stretch region were assigned to *trans,trans-* and *cis,trans-* rotamers. Stark spectroscopy of the *trans,trans-* OH stretch band provided the *a*-axis inertial component of the dipole moment, namely μ_a = 0.62(7) D. The computed equilibrium dipole moment agrees with the expectation value determined from experiment, consistent with a semi-rigid $CH_3O\ddot{C}OH$ backbone computed *via* a potential energy scan at the B3LYP/cc-pVTZ level of theory, which reveals substantial conformer interconversion barriers of $\sim$17 kcal mol^{-1}.

1.1.5 Stark Spectroscopy of Open-shell Molecular Complexes

Electrophilic addition of the hydroxyl radical to the π-bond of acetylene produces, as an intermediate, the carbon-centered 2-hydroxy vinyl radical ($\Gamma_e = A'$; H$\dot{C}$=COH). Along the entrance channel to this reaction, the dipole-quadrupole interaction stabilizes a *T*-shaped, hydrogen bonded complex (OH-C_2H_2), whose zero-point level lies $\sim$2.7 kcal mol^{-1} below the separated reactants.[75–77] Moreover, this entrance channel complex is located behind a barrier $\sim$1 kcal mol^{-1} above the reactant asymptote. The *T*-shaped complex was formed in He droplets *via* the sequential pick-up and solvation of the monomer fragments.[31] Rovibrational Stark spectra were recorded for OH-C_2H_2 and several other hydroxyl containing complexes.[35]

A model Hamiltonian was developed to account for the Stark effect in these systems,[35] which all exhibit partial quenching of electronic angular momentum quantized along the OH bond axis. Matrix elements of the Stark Hamiltonian were derived for a parity-conserving Hund's case (a) representation. The spherical tensor operator formalism was employed so as to arrive at the most general solution, in which the permanent dipole moment has projections on all three inertial axes. Formulae for transition intensities were given for *a-*, *b-*, and *c*-type bands measured with either parallel or perpendicular laser polarization configurations. For these open-shell complexes, a Coriolis interaction of the form $\hat{J}_a\left(\hat{l}_a + \hat{s}_a\right)$ lifts the $\pm\omega$ degeneracy associated with the electronic angular momentum of the OH radical. This dramatically reduces the effect of the inertial asymmetry in

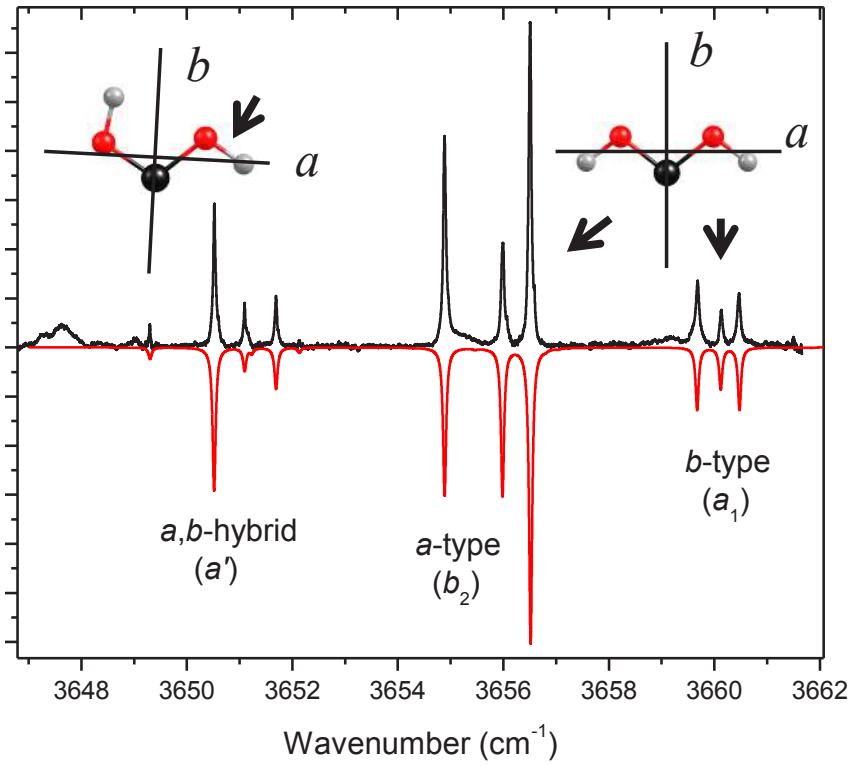

Figure 6: Rovibrational spectrum of *trans,trans*- and *cis,trans*-HOC̈OH rotamers in the OH stretch region. A simulation (red) derived from an asymmetric top Hamiltonian is shown below the experimental (black) spectrum. Assignments are based on band-types and nuclear spin statistical weights. Pure *b*- and *a*-type bands are observed for the symmetric and antisymmetric OH stretching vibrations of the C_{2v} *trans,trans*- rotamer, respectively. The *a,b*-hybrid band corresponds to the higher frequency OH stretch of the C_s symmetry *cis,trans*- rotamer.

these complexes, and in the absence of angular momentum quenching, all rotational levels exhibit a pseudo-first-order Stark effect. However, in the presence of angular momentum quenching, a subset of rotational levels is parity doubled, removing the degeneracy responsible for the linear Stark effect. Stark splitting of these parity doubled levels resembles the quadratic Stark effect expected for non-degenerate levels of a closed-shell asymmetric top. For the *T*-shaped OH-C_2H_2 complex, predictions of *a*- and *b*-type bands for a variety of Stark field strengths are in excellent agreement with experiment (see Fig. 7).

Experimental dipole moments obtained from Stark spectroscopy provide stringent benchmarks for electronic structure theory.[78–80] The quantum mechanical operator describing the dipole moment is a sum of one-electron operators, and its electronic expectation value converges rather quickly with increasing basis set size in a variational *ab initio* calculation.[81,82] Moreover, for systems that exhibit large-amplitude motion, the vibrational expectation value of the dipole moment provides a sensitive probe of the ground state nuclear wavefunction.[15,83] This was impressively

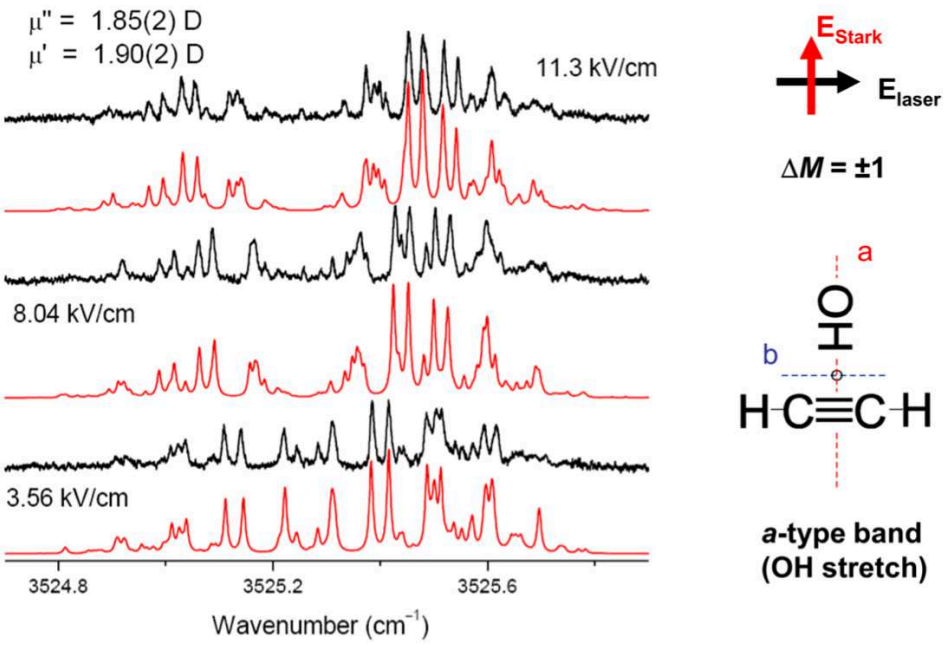

Figure 7: Experimental (black) and simulated (red) Stark spectra of the *a*-type OH stretch band of the OH-C_2H_2 complex. The laser polarization is aligned perpendicular to the Stark field axis. An effective Hamiltonian approach is employed to extract the permanent electric dipole moments from the spectra.[35]

demonstrated in a joint theoretical/experimental study by Douberly, Allen and co-workers.[15] Inertial dipole moment components of the hydridotrioxygen radical (*t*-HOOO) were probed with IR laser Stark spectroscopy, and these were shown to qualitatively disagree with vibrationally averaged values computed at the CCSD(T)/CBS level. The extent of dynamic correlation in this weakly bound radical system was found to be quite substantial, and agreement between experiment and theory was only obtained upon geometry optimization and vibrational averaging at the composite all-electron CCSDT(Q)/CBS level.[15] Indeed, we expect that Stark spectroscopy will continue to provide a general and powerful tool to probe the structural properties of molecular radicals and other species relevant to combustion chemistry.

1.1.6 Publications for which this DOE award was credited

1. Paul L. Raston, Tao Liang and Gary E. Douberly, "Infrared Spectroscopy and Tunneling Dynamics of the Vinyl Radical in ^{4}He Nanodroplets," *J. Chem. Phys.* **138**, 174302 (2013).

2. Paul L. Raston, Jay Agarwal, Justin M. Turney, Henry F. Schaefer III and Gary E. Douberly,"The Ethyl Radical in Superfluid Helium Nanodroplets: Rovibrational Spectroscopy and Ab Initio Computations," *J. Chem. Phys.* **138**, 194303 (2013).

3. Alexander M. Morrison, Paul L. Raston and Gary E. Douberly, "Rotational Dynamics of the Methyl Radical in Superfluid ^{4}He Nanodroplets," *J. Phys. Chem. A* **117**, 11640 (2013).

4. Christopher P. Moradi, Alexander M. Morrison, Stephen J. Klippenstein, C. Franklin Gold-

smith and Gary E. Douberly, "Propargyl + O_2 Reaction in Helium Droplets: Entrance Channel Barrier or Not?," *J. Phys. Chem. A* **117**, 13626 (2013).

5. Christopher M. Leavitt, Christopher P. Moradi, Bradley W. Acrey and Gary E. Douberly, "Infrared Laser Spectroscopy of the Helium-Solvated Allyl and Allyl Peroxy Radicals," *J. Chem. Phys.* **139**, 234301 (2013).

6. Christopher M. Leavitt, Christopher P. Moradi, John F. Stanton and Gary E. Douberly, "Communication: Helium Nanodroplet Isolation and Rovibrational Spectroscopy of Hydroxymethylene," *J. Chem. Phys.* **140**, 171102 (2014).

7. Bernadette M. Broderick, Laura McCaslin, Christopher P. Moradi, John F. Stanton and Gary E. Douberly, "Reactive Intermediates in ^{4}He Nanodroplets: Infrared Laser Stark Spectroscopy of Dihydroxycarbene," *J. Chem. Phys.* **142**, 144309 (2015).

8. Christopher P. Moradi and Gary E. Douberly, "On the Stark Effect in Open Shell Complexes Exhibiting Partially Quenched Electronic Angular Momentum: Infrared Laser Stark Spectroscopy of OH–C_2H_2, OH–C_2H_4, and OH–H_2O," *J. Mol. Spec.* **314**, 54 (2015).

9. Bernadette M. Broderick, Christopher P. Moradi and Gary E. Douberly, "Infrared Laser Stark Spectroscopy of Hydroxymethoxycarbene in ^{4}He Nanodroplets," *Chem. Phys. Lett.* **639**, 99 (2015).

10. Christopher P. Moradi, Changjian Xie, Matin Kaufmann, Hua Guo and Gary E. Douberly, "Two-center Three-electron Bonding in $ClNH_3$ Revealed via Helium Droplet Infrared Laser Stark Spectroscopy: Entrance Channel Complex along the Cl + NH_3 → $ClNH_2$ + H Reaction," *J. Chem. Phys.* **144**, 164301 (2016).

11. Matin Kauffman, Daniel Leicht, Martina Havenith, Bernadette M. Broderick and Gary E. Douberly, "Infrared Spectroscopy of the Tropyl Radical in Helium Droplets," *J. Phys. Chem. A* **120**, 6768 (2016).

12. Joseph T. Brice, Tao Liang, Paul L. Raston, Anne B. McCoy and Gary E. Douberly, "Infrared Stark and Zeeman Spectroscopy of OH-CO: The Entrance Channel Complex along the OH + CO → *trans*-HOCO Reaction Pathway," *J. Chem. Phys.* **145**, 124310 (2016).

13. Peter R. Franke, Daniel P. Tabor, Christopher P. Moradi, Gary E. Douberly, Jay Agarwal, Henry F. Schaefer III and Edwin L. Sibert III, "Infrared Laser Spectroscopy of the *n*-propyl and *i*-propyl Radicals: Stretch-Bend Fermi Coupling in the Alkyl CH Stretch Region," *J. Chem. Phys.* **145**, 224304, (2016).

14. Paul L. Raston, Emmanuel I. Obi, Gary E. Douberly, "Infrared Spectroscopy of the Entrance Channel Complex Formed Between the Hydroxyl Radical and Methane in Helium Nanodroplets" *J. Phys. Chem. A* **121**, 7597 (2017).

15. Alaina R. Brown, Peter R. Franke, Gary E. Douberly, "Helium Nanodroplet Isolation of the Cyclobutyl, 1-Methylallyl and Allylcarbinyl Radicals: Infrared Spectroscopy and Ab Initio Computations" *J. Phys. Chem. A* **121**, 7576 (2017).

2 References

[1] M. Y. Choi, G. E. Douberly, T. M. Falconer, W. K. Lewis, C. M. Lindsay, J. M. Merritt, P. L. Stiles, and R. E. Miller, *Int. Rev. Phys. Chem.* **25**, 15 (2006).

[2] J. P. Toennies and A. F. Vilesov, *Angew. Chem. Int. Ed.* **43**, 2622 (2004).

[3] J. P. Toennies, A. F. Vilesov, and K. B. Whaley, *Physics Today* **54**, 31 (2001).

[4] K. K. Lehmann and G. Scoles, *Science* **279**, 2065 (1998).

[5] F. Stienkemeier and K. K. Lehmann, *J. Phys. B: At. Mol. Opt. Phys.* **39**, R127 (2006).

[6] C. Callegari, K. K. Lehmann, R. Schmied, and G. Scoles, *J. Chem. Phys.* **115**, 10090 (2001).

[7] S. D. Flynn, D. Skvortsov, A. M. Morrison, T. Liang, M. Y. Choi, G. E. Douberly, and A. F. Vilesov, *J. Phys. Chem. Lett.* **1**, 2233 (2010).

[8] A. M. Morrison, S. D. Flynn, T. Liang, and G. E. Douberly, *J. Phys. Chem. A* **114**, 8090 (2010).

[9] T. Liang, S. D. Flynn, A. M. Morrison, and G. E. Douberly, *J. Phys. Chem. A* **115**, 7437 (2011).

[10] T. Liang and G. E. Douberly, *Chem. Phys. Lett.* **551**, 54 (2012).

[11] A. M. Morrison, J. Agarwal, H. F. Schaefer, and G. E. Douberly, *J. Phys. Chem. A* **116**, 5299 (2012).

[12] P. L. Raston, T. Liang, and G. E. Douberly, *J. Chem. Phys.* **137**, 184302 (2012).

[13] L. F. Gomez, R. Sliter, D. Skvortsov, H. Hoshina, G. E. Douberly, and A. F. Vilesov, *J. Phys. Chem. A* **117**, 13648 (2013).

[14] C. M. Leavitt, C. P. Moradi, B. W. Acrey, and G. E. Douberly, *J. Chem. Phys.* **139**, 234301 (2013).

[15] T. Liang, D. B. Magers, P. L. Raston, W. D. Allen, and G. E. Douberly, *J. Phys. Chem. Lett.* **4**, 3584 (2013).

[16] T. Liang, P. L. Raston, and G. E. Douberly, *ChemPhysChem* **14**, 764 (2013).

[17] C. P. Moradi, A. M. Morrison, S. J. Klippenstein, C. F. Goldsmith, and G. E. Douberly, *J. Phys. Chem. A* **117**, 13626 (2013).

[18] A. M. Morrison, T. Liang, and G. E. Douberly, *Rev. Sci. Inst.* **84**, 013102 (2013).

[19] A. M. Morrison, P. L. Raston, and G. E. Douberly, *J. Phys. Chem. A* **117**, 11640 (2013).

[20] E. I. Obi, C. M. Leavitt, P. L. Raston, C. P. Moradi, S. D. Flynn, G. L. Vaghjiani, J. A. Boatz, S. D. Chambreau, and G. E. Douberly, *J. Phys. Chem. A* **117**, 9047 (2013).

[21] P. L. Raston, J. Agarwal, J. M. Turney, H. F. Schaefer, and G. E. Douberly, *J. Chem. Phys.* **138**, 194303 (2013).

[22] P. L. Raston and G. E. Douberly, *J. Mol. Spec.* **292**, 15 (2013).

[23] P. L. Raston, T. Liang, and G. E. Douberly, *J. Phys. Chem. A* **117**, 8103 (2013).

[24] P. L. Raston, T. Liang, and G. E. Douberly, *J. Chem. Phys.* **138**, 174302 (2013).

[25] C. M. Leavitt, K. B. Moore, P. L. Raston, J. Agarwal, G. H. Moody, C. C. Shirley, H. F. Schaefer, and G. E. Douberly, *J. Phys. Chem. A* **118**, 9692 (2014).

[26] C. M. Leavitt, C. P. Moradi, J. F. Stanton, and G. E. Douberly, *J. Chem. Phys.* **140**, 171102 (2014).

[27] P. L. Raston, G. E. Douberly, and W. Jager, *J. Chem. Phys.* **141**, 044301 (2014).

[28] P. L. Raston, T. Liang, and G. E. Douberly, *Mol. Phys.* **112**, 301 (2014).

[29] B. M. Broderick, L. McCaslin, C. P. Moradi, J. F. Stanton, and G. E. Douberly, *J. Chem. Phys.* **142**, 144309 (2015).

[30] B. M. Broderick, C. P. Moradi, and G. E. Douberly, *Chem. Phys. Lett.* **639**, 99 (2015).

[31] G. E. Douberly, P. L. Raston, T. Liang, and M. D. Marshall, *J. Chem. Phys.* **142**, 134306 (2015).

[32] F. J. Hernandez, J. T. Brice, C. M. Leavitt, T. Liang, P. L. Raston, G. A. Pino, and G. E. Douberly, *J. Chem. Phys.* **143**, 164304 (2015).

[33] F. J. Hernandez, J. T. Brice, C. M. Leavitt, G. A. Pino, and G. E. Douberly, *J. Phys. Chem. A* **119**, 8125 (2015).

[34] C. P. Moradi and G. E. Douberly, *J. Phys. Chem. A* **119**, 12028 (2015).

[35] C. P. Moradi and G. E. Douberly, *J. Mol. Spec.* **314**, 54 (2015).

[36] C. P. Moradi, C. Xie, M. Kaufmann, H. Guo, and G. E. Douberly, *J. Chem. Phys.* **144**, 164301 (2016).

[37] M. Kuaffman, D. Leicht, M. Havenith, B. M. Broderick, and G. E. Douberly, *J. Phys. Chem. A* **120**, 678 (2016).

[38] J. T. Brice, T. Liang, P. L. Raston, A. B. McCoy, and G. E. Douberly, *J. Chem. Phys.* **145**, 124310 (2016).

[39] D. P. Franke, P. R. Tabor, C. P. Moradi, G. E. Douberly, J. Agarwal, H. F. Schaefer, and E. L. Sibert, *J. Chem. Phys.* **145**, 224304 (2016).

[40] R. Sliter, L. F. Gomez, J. Kwok, and A. Vilesov, *Chem. Phys. Lett.* **600**, 29 (2014).

[41] L. F. Gomez, E. Loginov, R. Sliter, and A. F. Vilesov, *J. Chem. Phys.* **135**, 154201 (2011).

[42] E. L. Knuth, B. Schilling, and J. P. Toennies. *International Symposium on Rarefied Gas Dynamics*, volume 19, pages 270–276 (Oxford University Press, Oxford, UK, 1995).

[43] M. Lewerenz, B. Schilling, and J. P. Toennies, *Chem. Phys. Lett.* **206**, 381 (1993).

[44] M. Hartmann, R. E. Miller, J. P. Toennies, and A. Vilesov, *Phys. Rev. Lett.* **75**, 1566 (1995).

[45] D. M. Brink and S. Stringari, *Z. Phys. D Atom. Mol. Cl.* **15**, 257 (1990).

[46] P. L. Stiles, K. Nauta, and R. E. Miller, *Phys. Rev. Lett.* **90**, 135301 (2003).

[47] K. Nauta and R. E. Miller, *Phys. Rev. Lett.* **82**, 4480 (1999).

[48] M. Y. Choi, F. Dong, and R. E. Miller, *Philos. T. Roy. Soc. A* **363**, 393 (2005).

[49] M. Y. Choi and R. E. Miller, *J. Am. Chem. Soc.* **128**, 7320 (2006).

[50] F. Dong and R. E. Miller, *Science* **298**, 1227 (2002).

[51] G. E. Douberly and R. E. Miller, *J. Phys. Chem. B* **107**, 4500 (2003).

[52] W. Kong and J. Bulthuis, *J. Phys. Chem. A* **104**, 1055 (2000).

[53] W. Kong, L. S. Pei, and J. Zhang, *Int. Rev. Phys. Chem.* **28**, 33 (2009).

[54] K. J. Franks, H. Z. Li, and W. Kong, *J. Chem. Phys.* **110**, 11779 (1999).

[55] A. R. Sharma, B. J. Braams, S. Carter, B. C. Shepler, and J. M. Bowman, *J. Chem. Phys.* **130**, 174301 (2009).

[56] F. Dong, M. Roberts, and D. J. Nesbitt, *J. Chem. Phys.* **128**, 044305 (2008).

[57] D. J. Nesbitt and F. Dong, *Phys. Chem. Chem. Phys.* **10**, 2113 (2008).

[58] A. R. Sharma, J. M. Bowman, and D. J. Nesbitt, *J. Chem. Phys.* **136**, 034305 (2012).

[59] S. Davis, D. Uy, and D. J. Nesbitt, *J. Chem. Phys.* **112**, 1823 (2000).

[60] T. Haber, A. C. Blair, D. J. Nesbitt, and M. D. Schuder, *J. Chem. Phys.* **124**, 054316 (2006).

[61] D. Uy, S. Davis, and D. J. Nesbitt, *J. Chem. Phys.* **109**, 7793 (1998).

[62] J. D. DeSain, R. I. Thompson, S. D. Sharma, and R. F. Curl, *J. Chem. Phys.* **109**, 7803 (1998).

[63] J. X. Han, Y. G. Utkin, H. B. Chen, N. T. Hunt, and R. F. Curl, *J. Chem. Phys.* **116**, 6505 (2002).

[64] J. D. DeSain and R. F. Curl, *J. Mol. Spec.* **196**, 324 (1999).

[65] J. Pacansky, D. E. Horne, G. P. Gardini, and J. Bargon, *J. Phys. Chem.* **81**, 2149 (1977).

[66] J. Pacansky and H. Coufal, *J. Chem. Phys.* **72**, 3298 (1980).

[67] P. S. Thomas and T. A. Miller, *Chem. Phys. Lett.* **491**, 123 (2010).

[68] P. R. Schreiner, H. P. Reisenauer, F. C. Pickard, A. C. Simmonett, W. D. Allen, E. Matyus, and A. G. Csaszar, *Nature* **453**, 906 (2008).

[69] L. Koziol, Y. M. Wang, B. J. Braams, J. M. Bowman, and A. I. Krylov, *J. Chem. Phys.* **128**, 204310 (2008).

[70] G. Lapidus, D. Barton, and P. E. Yankwich, *J. Phys. Chem.* **70**, 407 (1966).

[71] G. Lapidus, D. Barton, and P. E. Yankwich, *J. Phys. Chem.* **70**, 1575 (1966).

[72] G. Lapidus, D. Barton, and P. E. Yankwich, *J. Phys. Chem.* **70**, 3135 (1966).

[73] G. Lapidus, P. E. Yankwich, and D. Barton, *J. Phys. Chem.* **68**, 1863 (1964).

[74] P. R. Schreiner and H. P. Reisenauer, *Angew. Chem. Int. Ed.* **47**, 7071 (2008).

[75] J. B. Davey, M. E. Greenslade, M. D. Marshall, M. I. Lester, and M. D. Wheeler, *J. Chem. Phys.* **121**, 3009 (2004).

[76] M. D. Marshall, J. B. Davey, M. E. Greenslade, and M. I. Lester, *J. Chem. Phys.* **121**, 5845 (2004).

[77] M. D. Marshall and M. I. Lester, *J. Chem. Phys.* **121**, 3019 (2004).

[78] D. Ajitha and S. Pal, *Chem. Phys. Lett.* **309**, 457 (1999).

[79] P. U. Manohar and S. Pal, *Chem. Phys. Lett.* **438**, 321 (2007).

[80] L. Ravichandran, D. Bhattacharya, N. Vaval, and S. Pal, *J. Chem. Sci.* **124**, 223 (2012).

[81] F. Jensen, *J. Chem. Phys.* **115**, 9113 (2001).

[82] F. Jensen, *J. Chem. Phys.* **117**, 9234 (2002).

[83] M. Schnell, P. R. Bunker, G. von Helden, J. U. Grabow, G. Meijer, and A. van der Avoird, *J. Phys. Chem. A* **117**, 13775 (2013).